DOI 10.1007/s11141-020-10001-7
Radiophysics and Quantum Electronics, Vol. 62, Nos. 7–8, December, 2019
(Russian Original Vol. 62, No. 7–8, August–September, 2019)

LOW-NOISE SIS RECEIVERS FOR NEW RADIO-ASTRONOMY PROJECTS

K. I. Rudakov,[1,2,3] **P. N. Dmitriev,**[1] **A. M. Baryshev,**[1]
A. V. Khudchenko,[1,2] **R. Hesper,**[2] **and**
V. P. Koshelets[1*]

UDC 520.8.056

We have developed, manufactured, and tested a waveguide mixer in the range 211–275 *GHz on the basis of the superconductor–insulator–superconductor (SIS) tunnel structures. The methods of manufacturing high-quality tunnel structures on quartz substrates have been worked out. To extend the receiver band, the* $Nb/AlO_x/Nb$ *and* $Nb/AlN/NbN$ *tunnel junctions with a high current density of up to 20* kA/cm^2 *are employed. The dependence of the characteristics of the receiving elements on the signal frequency is simulated for the intermediate-frequency band* 4–12 *GHz. The measurements demonstrate a good agreement of the input band of the receiving structures with the calculated results. The uncorrected noise temperature of the receiver amounts to 24 K at a frequency of 265 GHz, which is only two times higher than the quantum limit. The receivers under development are intended for a number of newly-built ground-based radio telescopes ("Suffa" and LLAMA), as well as for the "Millimetron" space program.*

1. INTRODUCTION

In recent years, the possibility of creating devices with record-breaking parameters has been the main impetus for rapid development of superconductor electronics. This is explained by both extremely high nonlinearity of superconducting elements and their ultimately low natural noise, which is stipulated by their nature and cryogenic operation temperature. The development of the supersensitive terahertz receiving devices is one of the most successfully directions. The mixers on the basis of the superconductor–insulator–superconductor (SIS) tunnel junctions are definitely the best input devices for coherent receivers at the frequencies in the range from 0.1 to 1.2 THz since their noise temperature is restricted only by the quantum limit. At present, the heterodyne SIS receivers are used as standard units in the majority of both ground-based and space-borne radio telescopes all over the world [1–10]. In particular, the SIS receivers are successfully operated in all high-frequency ranges of the greatest contemporary radio-astronomy project, namely, the multielement interferometer ALMA (Atacama Large Millimeter/Submillimeter Array).

The SIS receivers have successfully been used not only on the Earth, but also onboard spacecraft. For example, the heterodyne instrument HIFI (Heterodyne Instrument for the Far Infrared) has quite recently been operated as part of the Herschel space observatory [11]. At present, several space missions including the project "Millimetron" of the Russian Space Agency are under development [12]. The "Millimetron" observatory is aimed at studying astronomic objects in the Universe in the far infrared, submillimeter, and millimeter ranges of the electromagnetic spectrum with superhigh sensitivity in the single-telescope regime

* valery@hitech.cplire.ru

[1] V. A. Kotel'nikov Institute of Radioengineering and Electronics of the Russian Academy of Sciences, Moscow, Russia; [2] Astronomical Institute, University of Groningen, Groningen, The Netherlands; [3] Moscow Physico-Technical Institute, Dolgoprudny, Russia. Translated from Izvestiya Vysshikh Uchebnykh Zavedenii, Radiofizika, Vol. 62, No. 7–8, pp. 613–622, August–September 2019. Original article submitted May 14, 2019; accepted July 5, 2019.

and an extremely high angular resolution in the regime of the ground-based and space-borne interferometer. The whole series of the heterodyne receiving systems with sensitivity close to the quantum limit should be developed to solve the research problems of the project. The range 211–275 GHz will be used for both operation in the regime of a space–Earth space-borne interferometer and a high-resolution (exceeding 10^6) spectrometer in the single-telescope regime (for which the required noise temperature is lower than 45 K in the two-band regime, the intermediate-frequency band is 4–12 GHz, and the spectral resolution is better than 1 MHz). The topicality of this range was confirmed by publishing the "image" of the supermassive black hole at the center of the M87 galaxy for the first time in history (the measurements were performed at a frequency of 230 GHz). The black hole at the center of our galaxy (the Sagittarius A radio source) and many other supercompact objects should be the next in turn. These studies are performed within the framework of the EHT (Event Horizon Telescope) project. New facilities for the superlong-base interferometry, including the LLAMA (Large Latin American Millimeter Array) and the Russia–Uzbekistan radio telescope "Suffa," are being developed.

In this work, we report on the results of the development and the first measurements of the characteristics of an SIS receiver with the range 211–275 GHz, which have been conducted by the researchers of V. A. Kotel'nikov Institute of Radioengineering and Electronics of the Russian Academy of Sciences jointly with the colleagues from Astronomical Institute, University of Groningen (The Netherlands). To realize the ultimate parameters of the SIS mixers, one should develop and optimize a repeatable and reliable technology for creating tunnel nanostructures with a tunnel-barrier thickness of about 1 nm with an extremely high current density and small leakage currents. The technology of creating such structures was developed and tested in V. A. Kotel'nikov Institute of Radioengineering and Electronics of the Russian Academy of Sciences.

The SIS-mixer structure and the methods for creating the receiving SIS structures and their manufacturing technology are described in Sec. 2. The knee-shaped feature, which appears in the current–voltage characteristic of the SIS junctions and its influence on the SIS-mixer operation is discussed in Sec. 3. The experimental methods for studying the SIS mixers and the results of measuring the noise characteristics of the SIS receiver are described in Sec. 4. Conclusions are given in Sec. 5.

2. THE SIS-MIXER CONSTRUCTION AND THE METHODS FOR MANUFACTURING RECEIVING SUPERCONDUCTOR STRUCTURES

The SIS tunnel junction on the basis of niobium films, which was manufactured on a 125 μm-thick quartz substrate, was used as the receiving element. To reach the low noise temperature, one should compensate for the large capacitance of the SIS junction in the operation frequency range and match its impedance at a high frequency (about 20–40 Ω) with the waveguide impedance about 400 Ω. This was reached by including the SIS junction in the planar structure which consisted of segments of coplanar and microstrip $Nb/SiO_2/Nb$ lines. Such a structure allowed one to compensate for the junction capacitance at the operation frequency and match the resulting low impedance with the waveguide. Although the sample is located in a metal channel and is a dielectric waveguide with a cutoff frequency exceeding 280 GHz, the waveguide line, which was formed by the niobium electrode and the waveguide wall, supports the steady-state mode in the range 211–275 GHz. To rule out the high-frequency signal leakage through the sample structure, the high-frequency rejection filters were located on its surface. Figure 1*a* shows a three-dimensional design model of a mixing element.

The waveguide receiving element was located in a rectangular waveguide with the dimensions 500×1000 μm orthogonally to the wave-propagation plane at a distance of 230 μm from the waveguide end. The mixing waveguide unit comprises the central part with the waveguide, the short-circuiting unit, the unit for specifying the magnetic field, and the input horn. Since at the intermediate frequency, the radiation wavelength is much longer than the planar-structure dimensions, the adjusting microstrip lines make a considerable capacitive contribution to the sample impedance at this frequency. The microstrip line located on an additional printed-circuit board with a dielectric constant of 9.8, was used for tuning the output

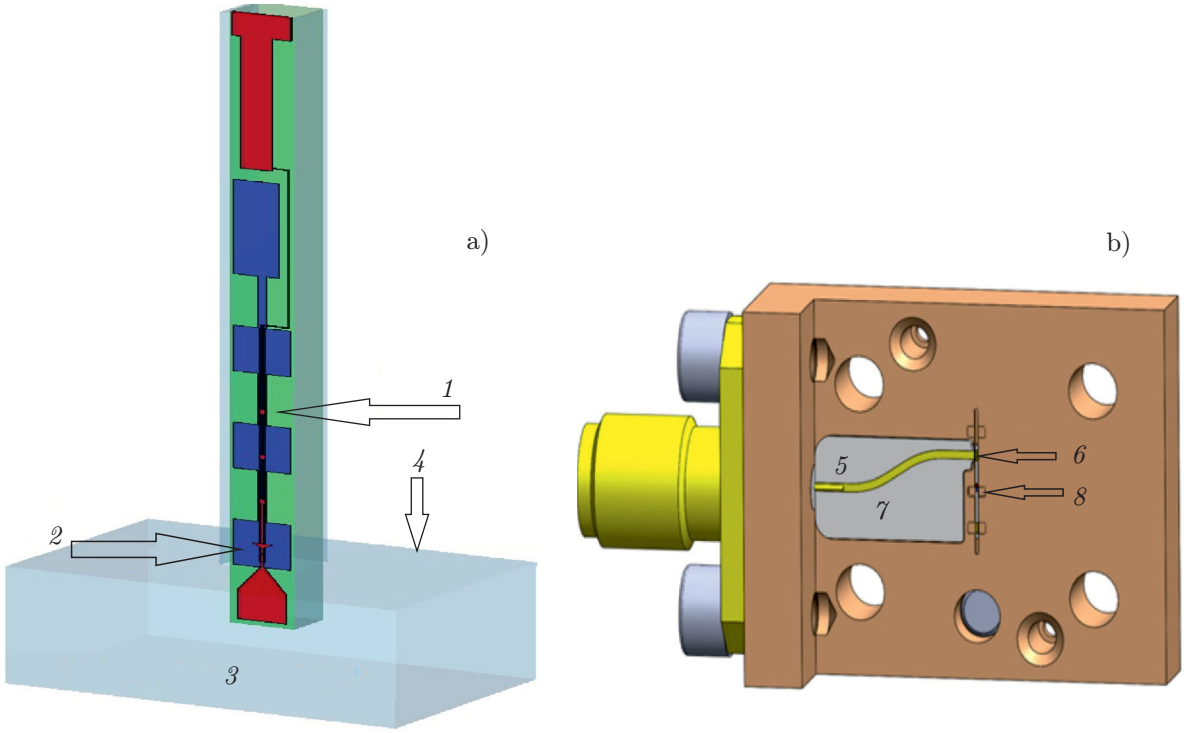

Fig. 1. The structure of the mixing element and the central part of the mixer unit. Panel *a*: three-dimensional model of the design of the mixing element with the dimensions $3250 \times 150 \times 125\,\mu$m located in the waveguide, high-frequency filter (*1*), SIS junction (*2*), waveguide input (*3*), and location of the short-circuiting wall (*4*). Panel *b*: three-dimensional model of a part of the mixing unit with the printed-circuit board for matching at the intermediate frequency (*5*). The unit comprises mixing element (*6*), behind which the short-circuiting plane is located in the waveguide, 50 Ω line (*7*), and the waveguide section (*8*) where the waveguide-connection region is also shown.

impedance of the mixing structure and its matching with the intermediate-frequency amplifier. Figure 1*b* shows a three-dimensional model of such a printed-circuit board (in the figure, the printed-circuit board contains only the line with a wave impedance of 50 Ω). Using the software package CST (Computer Simulation Technology), we have conducted full three-dimensional simulation of the manufactured structures, including the tuning elements and location of the sample chip in the waveguide. The numerical-simulation results are compared with the experimental data in Sec. 4.

To obtain the ultimately low noise temperatures of the receiver, one needs the junctions with small leakage currents. The ratio of the sub-gap resistance $R_{\rm sg}$ to the normal resistance $R_{\rm n}$ above the gap is the most widespread characteristic of the tunnel-junction quality for liquid-helium temperature (the required ratio is $R_{\rm sg}/R_{\rm n} > 25$, which is close to the ultimately possible value). In this work, we present the results for the SIS mixers on the basis of the Nb/Al-AlO$_x$/Nb junctions [13–15]. In these structures, the tunnel barrier is formed using the method of aluminum oxidation in the pure-oxygen medium. A thin aluminum (Al) film (the film thickness is $d \approx 5$–7 nm) uniformly covers the surface of niobium, ruling out its oxidation, and forms the homogeneous oxide Al_2O_3 on the surface. The Nb/Al-AlO$_x$/Nb junctions have some advantages over other types of SIS junctions: (i) small leakage currents; (ii) low specific capacitance (amounts to 0.05–0.08 pF/μm^2 depending on the current density); (iii) good parameter repeatability; and (iv) high stability to thermocycling and invariability of the tunnel characteristics in the process of long-term storage. The methods of manufacturing and characterization of the superconductor receiving structures on the basis of the niobium films have been developed and tested at V. A. Kotel'nikov Institute of Radioengineering and Electronics of the Russian Academy of Sciences [16–19].

The SIS junctions on the basis of the Nb/Al-AlO$_x$/Nb and Nb/Al-AlN$_x$/Nb structures were produced

using the selective niobium etching and anodization process (SNEAP) [15]. In what follows, the standard processing sequence of manufacturing the tunnel Josephson SIS junctions, which is successfully used at V. A. Kotel'nikov Institute of Radioengineering and Electronics of the Russian Academy of Sciences, is described.

The 125 μm-thick quartz plates are usually used as substrates and the standard dimensions of the substrate are 24×24 mm. The substrates are preliminarily cleaned in organic solvent (acetone), washed in distilled water, and dried by the compressed-air flow. The magnetron deposition of the Al_2O_3 buffer stop layer with a thickness of about 100 nm is then performed to exclude the substrate-material etching in the process of the junction formation by plasma chemical etching. Then the photoresist mask, which determines the base-electrode geometry for lift-off lithography, is formed on the substrate. The next stage involves deposition of the multilayered structure which determines the SIS-junction structure. The deposition is performed by the magnetron method in a single vacuum cycle using a facility by the "Kurt J. Lesker Company," which is equipped with a water-cooled substrate holder and the magnetron dc deposition systems operated at the radio frequency (rf) 13.56 MHz. The residual-gas pressure in the chamber amounts to $3 \cdot 10^{-8}$ mbar. First, a layer of 200 nm-thick lower niobium is deposited to be followed by a 7 nm-thick layer of barrier aluminum. Then the aluminum surface is oxidated in the pure-oxygen atmosphere and the upper niobium layer with a thickness of 50–100 nm is deposited. Niobium and aluminum were deposited by the method of reactive dc deposition in argon medium. Finally, to form the base electrode, the photoresist film, which is covered by the deposited multilayered structure, is removed from the circuit segments, which are not covered by the base electrode, in acetone or dimethylformamide by use of ultrasound (lift-off lithography).

Then direct formation of the SIS junctions was performed. The geometrical dimensions of the junctions are specified by the ultimate resolution of optical photolithography amounting to 0.4 μm, which allows one to obtain junctions with an area smaller than 1 μm^2. The junctions are formed by plasma chemical etching in the CF_4 medium by removing the upper niobium layer of the multilayered structure using the photoresist mask which determines the junction geometry. The AlO_x barrier is used as a stop layer, which stops the further etching of the structure. The plasma chemical etching is followed by anodizing in the ethylene glycol solution of ammonium pentaborate using the same photoresist mask, and the SiO_2 insulation layer, whose typical thickness amounts to 250 nm, is deposited by the rf magnetron method. Anodization is required to ensure a more reliable insulation over the SIS-junction perimeter to avoid possible short-circuiting between the base and the upper supplying electrodes in these regions. The opening of the contacts to the junctions is performed in dimethylformamide by the method of lift-off lithography. The upper supplying electrode is also formed by deposition of the niobium layer with the thickness in the range 300–500 nm using the lift-off lithography and the photoresist mask with its further removal in solvents. A similar method is used for forming the regions of the contact pads, for which gold is usually used as their material.

3. CURRENT–VOLTAGE CHARACTERISTICS OF AN SIS MIXER

The current–voltage characteristic (CV) of an SIS mixing Nb/Al-AlO_x/Nb element with an area of 1 μm^2 is shown in Fig. 2 by a solid curve. The CV is measured in the voltage-specification regime and the critical current of the SIS junction is suppressed by a magnetic field. The normal resistance of the SIS junction is $R_n = 38\ \Omega$, the quality parameter, which is the ratio of the resistances under and above the gap, is $R_{sg}/R_n = 28$, the gap voltage is $V_g = 2.83$ mV, and the smearing of the gap voltage is $\delta V_g = 0.3$ mV. It is of interest to observe a well-pronounced knee-shaped feature, which appears in the CV for voltages slightly higher than V_g. It is due to the presence of a normal aluminum layer near the tunnel barrier, which considerably modifies the electron-state density in a superconducting electrode. A theoretical model of such a structure [20] is developed on the basis of solving the quasiclassical Uzadel equations under the conditions of the so-called dirty limit, when the electron mean free-path length in a normal metal and a superconductor is much shorter than their coherence lengths, i.e., the films are sufficiently thick. The dependence of the effect on the tunnel-structure parameters was experimentally studied in [17].

If the tunnel junction is subject to the action of local-oscillator signal with frequency $f_{\rm LO}$, the quasi-particle steps [1, 2], whose size $\Delta V_{\rm qp}$ in terms of voltage is determined by the local-oscillator frequency $f_{\rm LO}$, appear in the CV: $\Delta V_{\rm qp} = \hbar f_{\rm LO}/e$ ($\hbar$ is Planck's constant and e is the elementary charge). The step increases from the gap voltage, such that for the frequency 265 GHz we have $\Delta V_{\rm qp} = 1.095$ mV. The experimental CV under the action of the local oscillator with a frequency of 265 GHz and the power $\alpha = 1$ (where $\alpha = eV_{\rm RF}/(\hbar f_{\rm LO})$ and $V_{\rm RF}$ is the radio-frequency signal voltage) [1, 2], which is optimal for the SIS mixer operation, is shown in Fig. 2 by a dash–dot line. When the local-oscillator signal is applied, the knee-shaped feature is significantly suppressed, but its presence can influence the SIS-mixer operation.

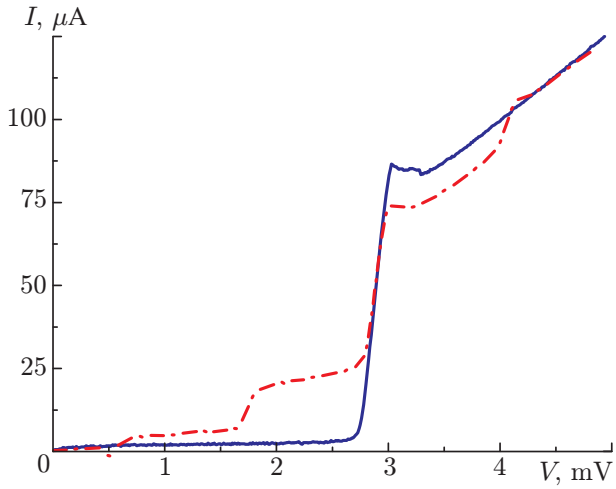

Fig. 2. Experimental CV of the mixing element: the solid curve shows an autonomous CV and the dash–dot line presents the CV subjected to the local-oscillator influence at a frequency of 265 GHz for the optimal power.

The numerical study of the local-oscillator influence on the CV of the SIS junction was performed using the model described in [21], which allows us to obtain the CV that is close to the experimental one (see Fig. 3*a* in which the autonomous model CV and the CV under the influence of the local-oscillator signal, which was calculated by the Tucker–Feldman theory [2], are shown). The calculations show that the presence of a knee-shaped feature leads to the appearance of a decreasing segment on the step (see Fig. 3*b*) even without allowance for the impedance of an external electrodynamic

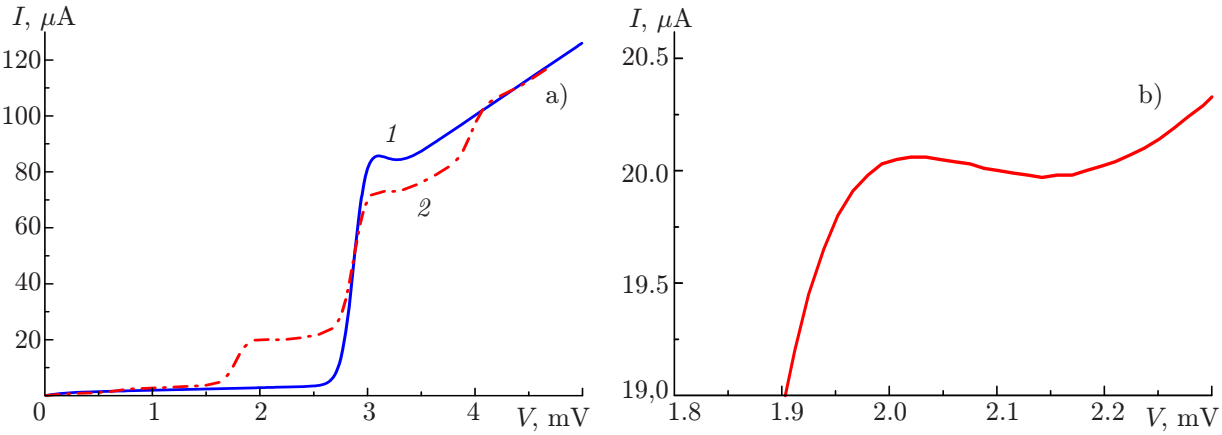

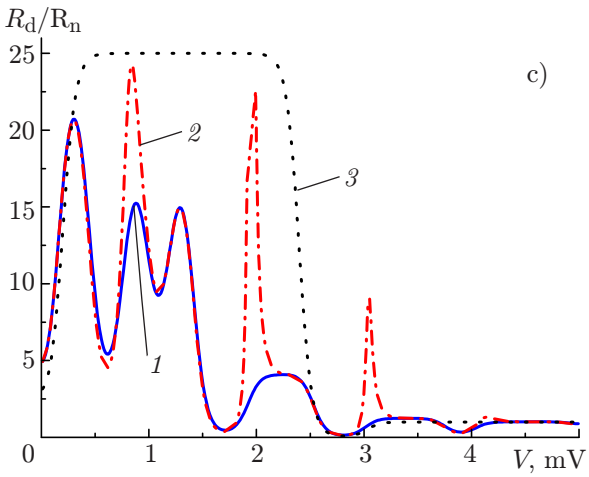

Fig. 3. Calculated characteristics of the mixing element: model CV (*a*) with the knee-shaped feature ($\gamma = 0.27$; curve *1*) and under the local-oscillator influence at 265 GHz with the optimal power $\alpha = 1$ (*2*), CV fragment in the region of the first quasiparticle step (*b*), and the dependence of the differential resistance $R_{\rm d}$ normalized to $R_{\rm n}$ (*c*) at the optimal local-oscillator power ($\alpha = 1$) for the junction without a pronounced knee-shaped feature ($\gamma = 0.05$; curve *1*), for the model curve that is close to the experiment ($\gamma = 0.27$; curve *2*), and for the autonomous SIS junction without the knee ($\alpha = 0$ and $\gamma = 0.05$; curve *3*).

system. The presence of a decreasing segment leads to large values of the differential resistance (see Fig. 3*c* in which the calculated dependences of the differential resistance normalized to the normal resistance of the junction are shown), which can significantly influence the SIS-mixer operation process, considerably reducing the voltage range of its effective operation. The calculated dependence, which was obtained for the model CV without the knee-shaped feature (the γ parameter, which characterizes the knee size in the model, has been reduced from 0.27 to 0.05) is shown in Fig. 3*c* by a solid line for comparison. The dotted line in this figure shows the dependence of the differential resistance, which was obtained for the autonomous CV of the SIS junction without the knee-shaped feature. The experimental measurements of the characteristics of a sample installed in the SIS mixer have shown that the influence of the knee-shaped feature turns out to be significantly weaker compared with the model calculations, and the cause of this discrepancy will be studied in what follows.

4. MEASUREMENT OF THE AMPLITUDE–FREQUENCY AND NOISE CHARACTERISTICS OF AN SIS RECEIVER

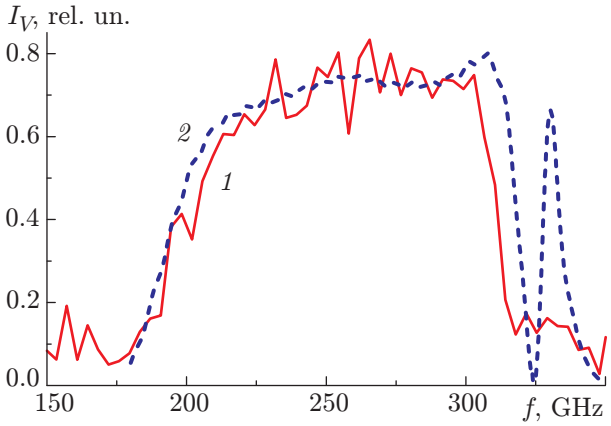

Fig. 4. Experimentally measured response I_V of the receiving SIS structure (the signal that is proportional to the SIS-junction current for the voltage slightly lower than the gap one), which was obtained using the Fourier-transform spectroscopy (curve *1*) and the calculated response (*2*) as functions of the frequency.

The receiving-element response was experimentally measured using a Michelson Fourier-transform interferometer. The resistive Globar heater was used as a broadband source of subterahertz radiation. To measure the receiving-element response, the voltage working point 2.5 mV (slightly below the gap voltage) was specified on the SIS junction. The results of Fourier-transform spectroscopy (FT) are shown in Fig. 4 (curve *1*). To ensure good suppression of the critical current of the tunnel junctions, the second or even the third minimum of the critical-current dependence on the external magnetic field was usually chosen. The critical-current suppression becomes better and electric noise becomes lower with increasing order of the minimum of the critical-current dependence on the external magnetic field. However, a large magnetic field decreases the superconductor energy gap, which leads to a decrease in the gap voltage in the CV. The measured response dependences on the frequency are in good agreement with the results of the mixer simulation using the CST (curve *2* in Fig. 4). When calculating the theoretical response, the parameters of the SIS element, which were obtained on the basis of its CV, were used in the model. The resonance at a frequency of 325 GHz is due to excitation of the waveguide mode in a quartz substrate with a thickness of 125 μm, which is located in a metal channel. This resonance is much higher than the operation frequency of the receiver and does not influence its operation in the range 211–275 GHz. It should be noted that since calculation of the entire structure with allowance for the superconducting properties of niobium requires considerable time, the simulation was performed for the fundamental mode of the waveguide in the frequency range from 150 GHz (the cutoff frequency of the TE_{10} mode) to 300 GHz (the second-mode frequency). The calculation for the higher frequencies is not rigorous because of a decrease in accuracy within the framework of the used model for the frequencies exceeding 305 GHz.

The noise temperature was measured by the standard Y-factor method and the absorber at a temperature of 295 K was used as a “hot” load, while the absorber cooled to 78 K was used as a “cold” load. Figure 5 shows the dependences of the output signal of the SIS receiver on the bias voltage, which were measured for the local-oscillator frequency 265 GHz at the intermediate frequency 6.5 GHz (the bandwidth of the intermediate-frequency filter is 40 MHz). The responses for the cold and warm loads at the input are

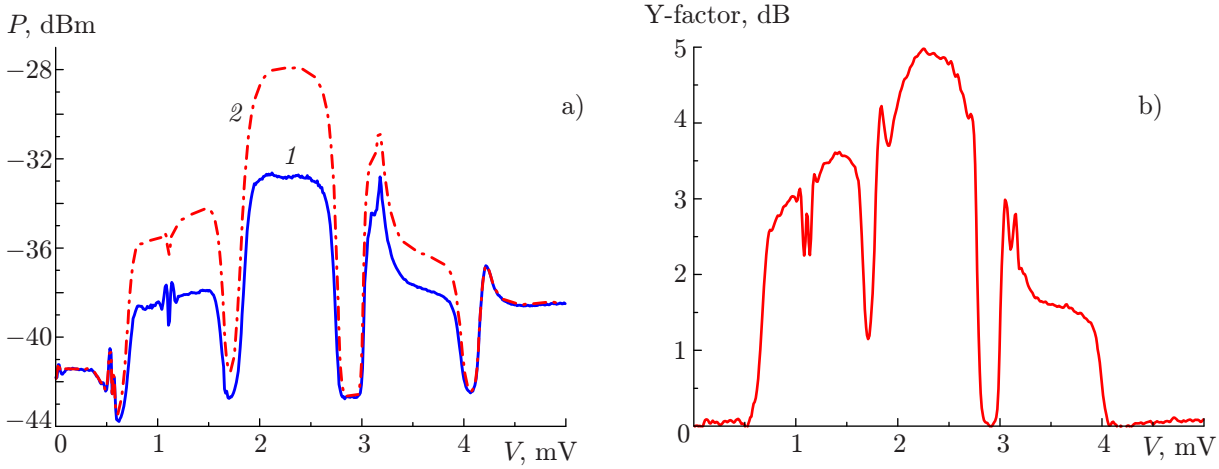

Fig. 5. Dependences of the output signal P of the SIS receiver on the bias voltage, measured at the intermediate frequency 6.5 GHz for the cold (curve *1*) and warm (*2*) input loads, for the local-oscillator frequency 265 GHz (*a*) and the Y-factor dependence on the bias voltage obtained from Fig. 5*a* (*b*).

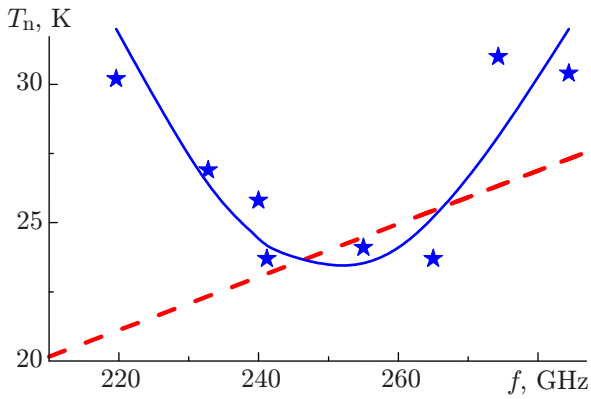

Fig. 6. The frequency dependence of the double-sideband noise temperature T_n for the SIS receiver. The experimental values are presented without corrections for losses in the beam splitter and the input window of a cryostat.

shown by curves *1* and *2*, respectively. Figure 5*b* shows the Y-factor dependence on the bias voltage. At the best points, the Y-factor values actually reach 5 dB, which corresponds to the receiver noise temperature 24 K. The dependence of the double-sideband noise temperature of the SIS receiver on the local-oscillator frequency is shown in Fig. 6. It should be noted that the experimental values are shown without corrections (the losses for the beam splitter, the input cryostat window, and the filters at the steps 78 and 4.2 K were not subtracted). The obtained values of the noise temperature only a factor of two exceed the quantity $\hbar f/k_B$ (k_B is Boltzmann's constant) and satisfy the technical requirements for the receiver operated in the range 211–275 GHz for the receiving complex of the space radio telescope "Millimetron."

Note that two local oscillators were used for the measurements. Instabilities in the output intermediate-frequency signal, which were related to both nonoptimal values of the impedance of the external electrodynamic system at these frequencies and the presence of the knee-shaped feature, emerged at some values of the local-oscillator frequency. The data shown in Figs. 5 and 6 have been obtained at an intermediate frequency of 6.5 GHz. The dependences of the output signal of the SIS receiver on the intermediate frequency, which were measured for the cold and warm loads at the input, are shown in Fig. 7*a* and the corresponding dependence of the noise temperature of the SIS receiver on the intermediate frequency is given in Fig. 7*b*. In the first experiments, no additional matching structures were installed on the intermediate-frequency matching board, and a uniform microstrip line with the wave impedance 50 Ω was used. This explains the irregularity with respect to the intermediate frequency and an increase in the noise temperature at high frequencies.

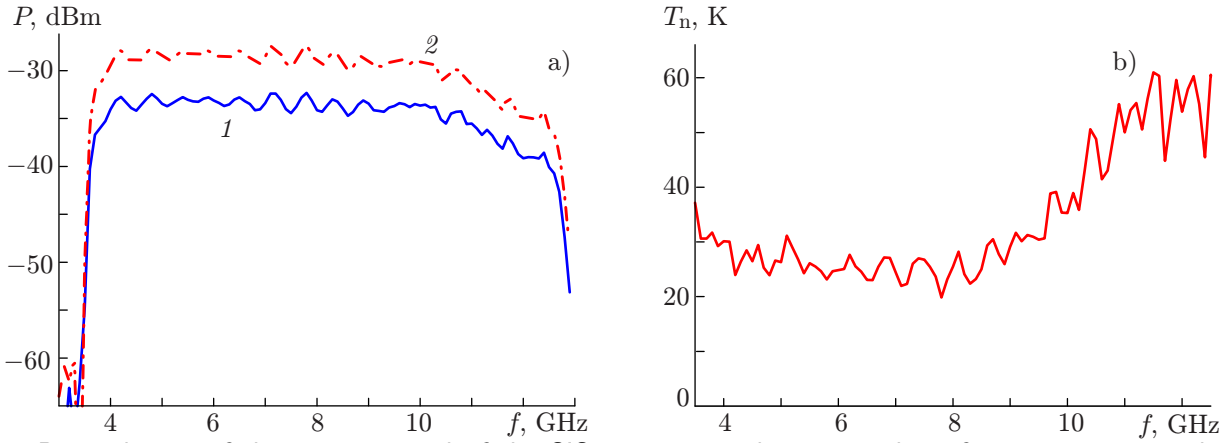

Fig. 7. Dependences of the output signal of the SIS receiver on the intermediate frequency, measured at a local-oscillator frequency of 265 GHz for the cold (curve *1*) and warm (curve *2*) loads at the input (*a*) and the dependence of the noise temperature of the SIS receiver on the intermediate frequency (*b*).

5. CONCLUSIONS

The receiving elements in the range 211–275 GHz have been developed, fabricated, and preliminarily studied. The experimentally measured minimum noise temperature of the receiver amounts to 24 K, which only a factor of two exceeds the quantum limit $\hbar f/k_{\mathrm{B}}$. The created receivers are intended for some developed ground-based radio telescopes ("Suffa" and LLAMA), as well as for the space project "Millimetron." Sideband separation receivers should be developed for use in actual radio telescopes. The development of such a device and optimization of the intermediate-frequency channel will be our next step. It is noteworthy that the mixer structure described in this work employs the approach, which has already been evaluated in the receiving complex ALMA (Chile), and the mixer tested in this work can be used as a part of a sideband separation receiver.

This work was supported by the Russian Science Foundation (contract No. 19–19–00618). The tunnel junctions were manufactured at V. A. Kotel'nikov Institute of Radioengineering and Electronics of the Russian Academy of Sciences within the framework of the state assignment using the unique scientific facility No. 352529.

REFERENCES

1. J. R. Tucker, *IEEE J. Quantum Electron.*, **15**, No. 11, 1234 (1979).
2. J. R. Tucker and M. J. Feldman, *Rev. Mod. Phys.*, **57**, No. 4, 1055 (1985).
3. J. W. Kooi, M. Chan, T. G. Phillips, et al., *IEEE Trans. Microwave Theory Tech.*, **40**, No. 5, 812 (1992).
4. A. Karpov, J. Blondell, M. Voss, and K. H. Gundlach, *IEEE Trans. Appl. Supercond.*, **5**, No. 2, 3304 (1995).
5. B. D. Jackson, G. de Lange, T. Zijlstra, et al., *IEEE Trans. Microwave Theory Tech.*, **54**, No. 2, 547 (2006).
6. A. Karpov, D. Miller, F. Rice, et al., *IEEE Trans. Appl. Supercond.*, **17**, No. 2, 343 (2007).
7. A. R. Kerr, S. K. Pan, S. M. X. Claude, et al., *IEEE Trans. Terahertz Sci. Technol.*, **4**, No. 2, 201 (2014).
8. A. M. Baryshev, R. Hesper, F. P. Mena, et al., *Astron. Astrophys.*, **577**, A129 (2015).
9. Y. Uzawa, Y. Fujii, A. Gonzalez, et al., *IEEE Trans. Appl. Supercond.*, **25**, No. 3, 2401005 (2015).
10. A. Khudchenko, A. M. Baryshev, K. Rudakov, et al., *IEEE Trans. Terahertz Sci. Technol.*, **6**, No. 1, 127 (2016).

11. Th. de Graauw, F. P. Helmich, T. G. Phillips, et al., *Astron. Astrophys.*, **518**, L6 (2010).
12. A. V. Smirnov, A. M. Baryshev, P. de Bernardis, et al., *Radiophys. Quantum Electron.*, **54**, Nos. 8–9, 557 (2011).
13. M. Gurvitch, W. A. Washington, and H. A. Huggins, *Appl. Phys. Lett.*, **42**, No. 5, 472 (1983).
14. H. A. Huggins, *J. Appl. Phys.*, **57**, No. 6, 2103 (1985).
15. H. Kroger, L. N. Smith, and D. W. Jillie, *Appl. Phys. Lett.*, **39**, No. 3, 280 (1981).
16. V. P. Koshelets, S. A. Kovtonyuk, I. L. Serpuchenko, et al., *IEEE Trans. Magn.*, **27**, No. 2, 3141 (1991).
17. P. N. Dmitriev, A. B. Ermakov, and A. G. Kovalenko, *IEEE Trans. Appl. Supercond.*, **9**, No. 2, 3970 (1999).
18. L. V. Filippenko, S. V. Shitov, and P. N. Dmitriev, *IEEE Trans. Appl. Supercond.*, **11**, No. 1, 816 (2001).
19. P. N. Dmitriev, I. L. Lapitskaya, L. V. Filippenko, et al., *IEEE Trans. Appl. Supercond.*, **13**, No. 2, 107 (2003).
20. A. A. Golubov, E. P. Houwman, J. G. Gijsbertsen, et al., *Phys. Rev. B*, **51**, No. 2, 1073 (1995).
21. S. V. Shitov, "Integral devices on superconductor tunnel junctions for the millimeter- and submillimeter-wave receivers," D. Sci. Thesis [in Russian], V. A. Kotel'nikov Institute of Radioengineering and Electronics of the Russian Academy of Sciences, Moscow (2003).